NANO LETTERS

Letter

pubs.acs.org/NanoLett

Thermal Rectification in Three-Dimensional Asymmetric Nanostructure

Jonghoon Lee,*[,†,‡] Vikas Varshney,[†,‡] Ajit K. Roy,[†] John B. Ferguson,[†] and Barry L. Farmer[†]

[†]Materials and Manufacturing Directorate, Air Force Research Laboratory, Wright-Patterson Air Force Base, Ohio 45433, United States

[‡]Universal Technology Corporation, 1270 N. Fairfield Road, Dayton, Ohio 45432, United States

ABSTRACT: Previously, thermal rectification has been reported in several low-dimensional shape-asymmetric nanomaterials. In this Letter, we demonstrate that a three-dimensional crystalline material with an asymmetric shape also displays as strong thermal rectification as low-dimensional materials do. The observed rectification is attributed to the stronger temperature dependence of vibration density of states in the narrower region of the asymmetric material, resulting from the small number of atomic degrees of freedom directly interacting with the thermostat. We also demonstrate that the often reported "device shape asymmetry" is not a sufficient condition for thermal rectification. Specifically, the size asymmetry in boundary thermal contacts is equally important toward determining the magnitude of thermal rectification. When the boundary thermal contacts retain the same size asymmetry as the nanomaterial, the overall system displays notable thermal rectification, in accordance with existing literature. However, when the wider region of the asymmetric nanomaterial is partially thermostatted by a smaller sized contact, thermal rectification decreases dramatically and even changes direction.

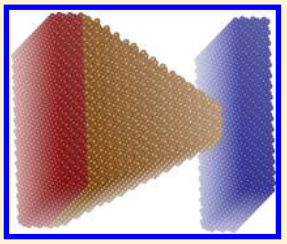

KEYWORDS: *Thermal rectifier, phonon density of states, central limit theorem, molecular dynamics*

Since the seminal experimental work by Chang et al. measured a small, but definite, thermal rectification in asymmetrically mass-loaded nanotubes,[1] directed thermal transport in nanostructured materials has been attracting significant scientific attention.[2] A small-scale solid state thermal rectifier, as an ideal component for thermal logic circuits, should revolutionize thermal management and energy efficiency in a broad gamut of applications. However, there are two major challenges to overcome for these promises to be realized.

The first challenge lies in the necessity of nanofabrication technologies with atomistic rigor and the characterization of thermal properties at nanoscale (~10 nm).[2] The rarity of experimental contributions in this subject is a direct consequence of this formidable challenge. Nonetheless, multiple complementary modeling efforts have reported promising forecasts of thermal rectification in nanodevices. Most of these studies involve a certain shape or mass asymmetry in low-dimensional nanostructures, such as carbon nanotubes, graphene sheets, nanohorns, and nanocones.[3−6]

The other challenge lies in our lack of understanding of the thermal rectification mechanism in studied nanostructured materials.[2] Although Chang et al. suspected solitons to be responsible for the observed rectification,[1] the mechanism is still a subject of controversy. A modeling effort to replicate the experimental observation resulted in a perplexing outcome.[7] Alaghemandi et al. performed a reverse nonequilibrium molecular dynamics (Rev-NEMD) study on an asymmetrically mass loaded CNT, similar to the experiment by Chang et al., and successfully observed a thermal rectification in similar magnitude to the experiment.[7] Peculiarly though, the simulation study predicted a stronger flux in the direction from low-mass (thin) to high-mass (thick), which is in contrast to the experiment where the stronger heat flux was along the opposite direction. Although the mechanism is still being sought after, the simple, yet intriguing, concept of thermal rectification using shape asymmetry is being confirmed repeatedly by several NEMD studies.[3−6] In this Letter, we aim to provide a few insights toward understanding the mechanism of thermal rectification in asymmetric nanostructures by addressing two important issues in particular.

The first issue regards the structural choice for the thermal rectifier. While most simulation studies so far have been performed exclusively on low-dimensional nanomaterials, there is no fundamental reason behind such a preference. It is an interesting question whether any three-dimensional crystalline material would display comparable thermal rectification features, when studied under similar conditions of shape asymmetry. In fact, various probing tips of atomic force microscopes (AFM) and scanning tunneling microscopes (STM) are examples of already existing three-dimensional asymmetric nanostructures, which could be tested for possible thermal rectification.

The second issue is associated with the simulation methodology repeatedly adopted in the literature. In contrast to the experimental setup where the nanotube device was placed between two large thermal leads, that is, reservoirs,[1] most NEMD simulation studies place thermostats at the opposite end-regions of the asymmetric device itself, thus rendering the

Received: March 14, 2012
Revised: June 18, 2012

 © XXXX American Chemical Society dx.doi.org/10.1021/nl301006y | *Nano Lett.* XXXX, XXX, XXX−XXX

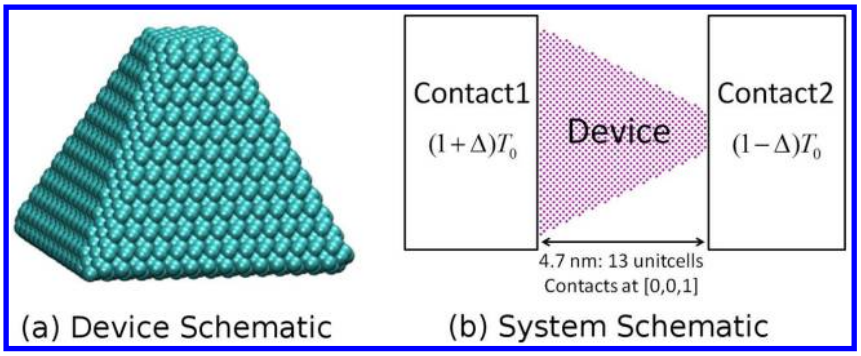

Figure 1. System schematics. (a) Shape of the diamond device. The bottom area is 34 nm^2 (16 unit cells × 16 unit cells). The height of the device is 4.7 nm (13 unit cells). Two different aspect ratios are studied with two different top areas of 0.52 nm^2 (2 unit cells × 2 unit cells) and 1.1 nm^2 (3 unit cells × 3 unit cells). (b) The device is placed between two contacts thermostatted at two different temperatures of $(1 + \Delta)T_0$ for Contact1 and $(1 - \Delta)T_0$ for Contact2 where T_0 is 200 K.

thermal contacts to be asymmetric as well.[3−6] An exception was the Rev-NEMD study by Alaghemandi et al., where the mass-graded CNT was placed between two symmetric boundary regions of bare CNT.[7] It is very important to notice the difference between the thermal contacts employed in experimental[1] and simulation setup.[7] While the energy exchange in simulation was performed between two narrow bare nanotube regions, the thermal leads in the experiment were much larger than the device itself. As we discuss later, such a difference in the size of thermal reservoirs results in a qualitatively different thermal rectification behavior, such as the reversal of the rectifying direction.

Because a fabricated asymmetric device has to be placed between two thermal leads to perform or to be tested experimentally, it becomes a reasonable question to ask whether to treat the thermal leads as an integral part of the proposed rectifying system. One might argue that the exclusion of thermal reservoirs from the system of interest, as adopted in many NEMD studies, is the way to study the intrinsic material property of the device. However, we believe that if device performance is qualitatively affected by the shape and size of boundary thermal reservoirs, then the often predicted thermal rectification feature in an asymmetric nanostructure should not be considered an intrinsic material property.

In order to address the two issues discussed above, we choose three-dimensional single crystalline diamond as the model nanostructure, which is carved in a pyramid shape (Figure 1a). We cut the tip of the pyramid to make a flat surface that is always narrower than the base of the pyramid. In addition, instead of applying thermostats in the end-regions of the nanostructure device itself, we place the device between two thermal contact reservoirs (Figure 1b). To eliminate the issue of interface thermal resistance between the device and the thermal contact reservoirs, the contacts are also made of the same crystalline diamond and seamlessly attached to the device by covalent bonding. All simulations are performed using LAMMPS molecular dynamics package[8] while PCFF force field is used to evaluate all bonded and nonbonded atomic interactions.[9]

We vary the size of the two contacts to address the effect of the contact size on the performance of the thermal rectifier. As shown in Figure 2, three different cases of thermal contacts are studied. First, the same size asymmetry as that of the pyramid device is applied on the reservoirs (Figure 2a, LS-contact). In the other two cases, the device is placed between two small and large symmetric thermal reservoirs; SS-contact (Figure 2b) and

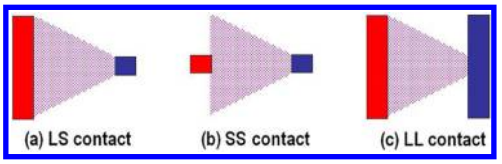

Figure 2. Systems with the same pyramid device but with different types of thermal contact sizes. (a) LS-contact: The thermal contacts retain the same size asymmetry of the device. (b) SS-contact: The surface area of two thermal contacts are the same, matched to the narrower (top) area of the device. (c) LL-contact: The thermal contacts are of the same size matched to the wider (bottom) area of the device. In all three cases, each thermal contact is 3 unit cells thick (≃1 nm). An additional single layer of atoms of fixed positions are attached at both ends of the system to suppress the center of mass movements of the thermostats.

LL-contact (Figure 2c) respectively. Here, "L" or "S" represents large or small size of thermal reservoir attached to the asymmetric nanostructure. However, from the perspective of the device-contact interface through which the device exchanges thermal energy with the reservoir, it should be noted that LS-contact and LL-contact are identical, because the interface area between the device and Contact2 is the same in both cases. Nevertheless, we discuss LL-contact separately later on to examine a numerical issue of the thermostat which distinguishes LL-contact from LS-contact in the practice of NEMD.

The temperature of the two thermal reservoirs is regulated using Nosé−Hoover thermostats. Whenever it is desired to maintain the integrity of the equilibrium in the ensemble of reservoir microstates, a due caution must be paid to the choice and optimization of the thermostat algorithm. However, in NEMD simulations, because a finite heat flux to and from the thermostats is always present, the equilibrium within the thermostat is constantly disturbed. In addition, it was recently observed that different thermostatting algorithms in NEMD simulations induce only negligible differences in the heat flux (less than 3%), where the device is strongly out of equilibrium at steady state due to a large temperature gradient.[10] Therefore, we believe that following results and discussion should be indifferent with regard to the thermostatting algorithm applied to the thermal reservoirs.

We discuss LS-contact first, as it presents a similar approach to previous NEMD studies in which thermostats are directly applied to the ends of the asymmetric device itself.[3−6] In LS-contact, the thermal contacts retain the same size asymmetry as

dx.doi.org/10.1021/nl301006y | *Nano Lett.* XXXX, XXX, XXX−XXX

that of the device. As shown in Figure 3a, the heat flux when Contact1 is held at the higher temperature, that is, $\Delta > 0$

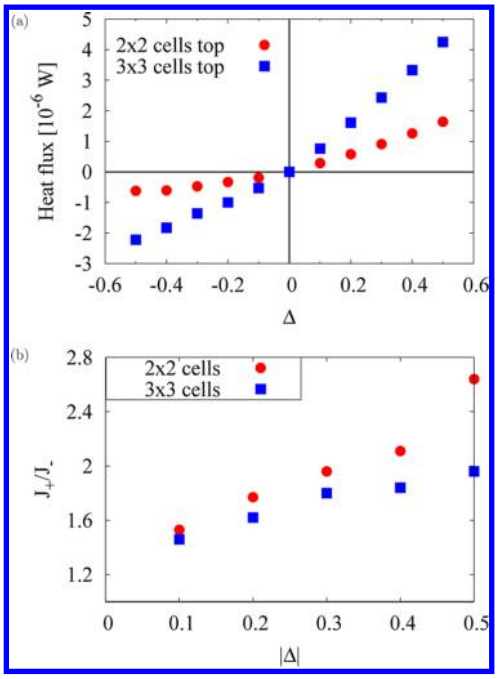

Figure 3. Thermal rectification in LS-contact. $J_{+(-)}$ is the heat flux when Δ is positive (negative). (a) Heat flux is weaker for the device with a narrower top area of 2 × 2 unit cells. (b) However, the rectification is stronger for the device with the stronger asymmetry. Errors are smaller than the size of symbols.

(Figure 1), is stronger compared to the heat flux when the temperature bias is reverted, suggesting that the system rectifies the heat flux along the wide to narrow direction. In addition, Figure 3b shows that the pyramid device with the stronger shape asymmetry shows the higher degree of thermal rectification. This is in agreement with previous findings reported for graphene ribbons and other low-dimensional devices.[3−6] Hence, it is evident from Figure 3 that given the asymmetric nature of thermal reservoir as in LS-contact, regular three-dimensional crystal materials do display noticeable thermal rectification when the requisite shape asymmetry is incorporated at the nanoscale.

A qualitative understanding of the mechanism behind this rectification can be obtained by analyzing the vibrational characteristics of the pyramid device for different applied temperature biases ($+\Delta$ and $-\Delta$). Because the asymmetric shape renders a nonuniform vibration density of states (vDOS) within the device, a simple comparison of the whole device vDOS for opposite Δ's would not provide significant insights as to how the sign of Δ affects the device vDOS. Therefore, we investigate the regional vDOS in the steady state using the velocity autocorrelation function defined as follows

$$vDOS(\omega) = \frac{1}{NT}\sum_{i}^{N}\sum_{\alpha}^{x,y,z}\hat{v}_{i,\alpha}^{\dagger}(\omega)\hat{v}_{i,\alpha}(\omega) \quad (1)$$

where N is the number of atoms in the region of interest and T is the average temperature of that region in steady state. $\hat{v}_{i,\alpha}$ and its conjugate, $\hat{v}_{i,\omega}^{\dagger}$ are the velocity of the ith atom along α direction in the frequency domain, ω, calculated from a discrete Fourier transform of the time domain velocity data sampled every 5 fs. Further block averaging of vDOS is done over 20 statistically independent blocks, each of which spans 7 ns.

Figure 4 compares vDOS of the wide and narrow regions within the pyramid device with LS-contact when $\Delta = +0.5$

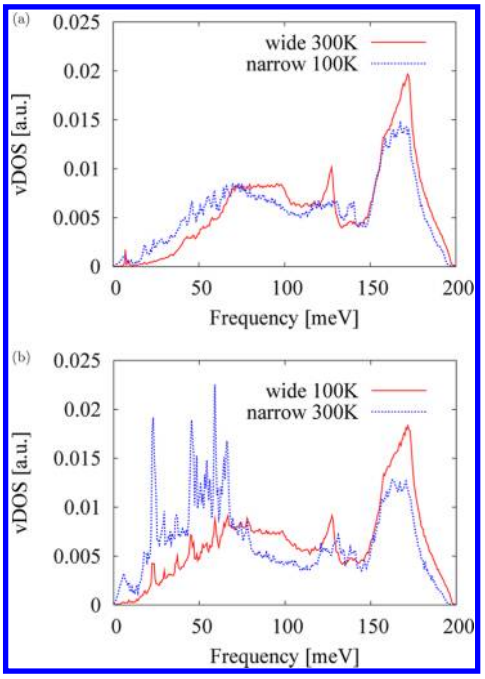

Figure 4. The vibrational density of states (vDOS) per atom for the LS-contact case. The pyramid device has 2 × 2 unit cells top. The vDOS of atoms close to wide contact agrees well with the experimental vDOS of bulk diamond when the frequency is lower than 180 meV.[11] (a) Δ is +0.5. (b) Δ is −0.5.

(Figure 4a) and $\Delta = -0.5$ (Figure 4b). Atoms used in the vDOS calculation are within the pyramid device but close to thermal contacts, such that they belong to the first two unit cells away from each contact. Atoms belonging to the thermal contacts are excluded from vDOS calculations, because their dynamics are constrained by the thermostat. Compared to the wide base, the narrow top is characterized by the larger surface (exposed to vacuum) to volume ratio, smaller number of atoms, and more importantly, the lesser number of atoms directly interacting with the thermal contact. Figure 4 displays the consequences of these three characteristics of narrow top on the vDOS. Figure 4a shows that the calculated vDOS of the wide base is very close to that of bulk diamond,[11] indicating negligible contributions from the surface atoms that are exposed to vacuum. On the contrary, the vDOS of the narrow top, because of a comparatively larger surface to volume ratio, displays significant surface phonon effects including phonon softening. Figure 4b presents an interesting observation taking place in the vDOS of the narrow top as the temperature bias is reversed ($\Delta < 0$); a few pronounced vibrational peaks appear in the frequency regime below 70 meV. Sharp peaks in vDOS indicate that the corresponding vibration modes are of standing wave nature. A close examination of the dynamics of the device atoms in the physical space shows that the low-frequency (<70 meV) peaks of Figure 4b correspond to the large-scale, yet localized, vibrations involving the whole narrow region and its center of mass. In all, it is clearly observed from Figure 4 that the vDOS of the narrow top region of the device is much more sensitive to the temperature change than that of the wide base

dx.doi.org/10.1021/nl301006y | Nano Lett. XXXX, XXX, XXX−XXX

region, resulting in a pronounced mismatch in vDOS when the narrow side is hotter than the wide side of the nanostructure, that is, when Δ is negative. It should be noted the observed emergence of low-frequency modes is not related to the so-called flying ice cube artifact frequently encountered in MD thermostats[12] as the Nosé−Hoover thermostat is used for the thermal reservoir, whose total translational and angular momentum are fixed to zero in our simulations.

The origin of the low-frequency peaks in Figure 4b is rather fundamental and related to the smallness of the device atomic degrees of freedom directly interacting with the thermal contact. Ideally, when an arbitrary device interacts with a thermal bath without rigid body motion, the total momentum transferred to the device from the thermal bath through device-contact interaction should always be zero since the kinetic energy corresponding to the center of mass (COM) degrees of freedom does not contribute to the temperature. However, such an ideal exchange of thermal energy between thermal bath and a nanoscale device is hard to be realized in practice, even harder in computer simulations, because the finite degrees of freedom participating in the device-contact interaction allow inevitable fluctuations in the net momentum exchanged. In MD simulations, the total momentum of a thermal reservoir composed of N_{bath} atoms can be artificially regulated to zero without affecting reservoir temperature. However, even when the whole reservoir is free of rigid body vibrations, a subsystem within the thermal reservoir would have a finite COM velocity fluctuating around zero. According to the central limit theorem,[13] the strength of this fluctuation is proportional to $(T/N_{sub})^{1/2}$, where N_{sub} is the number of atoms in the subsystem, and T is the reservoir temperature. For thermostats applied in the LS-contact case, this behavior is confirmed in Figure 5.

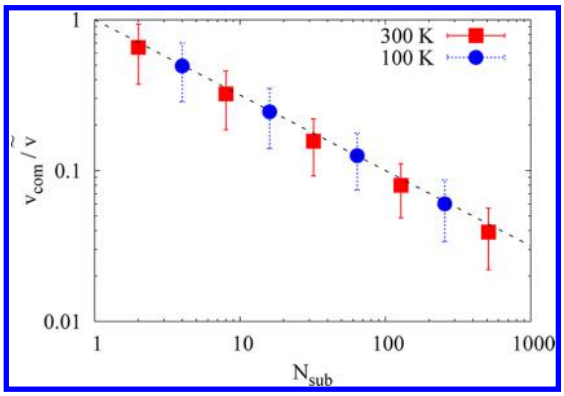

Figure 5. The center of mass velocity (v_{com}) of a subsystem composed of N_{sub} atoms within a thermal bath is plotted against N_{sub} for two different thermal bath temperatures. Contact1 of LS-contacts is used as the thermal bath. The dotted line shows the scaling of $N_{sub}^{-1/2}$. $\tilde{v} = (3k_BT/m)^{1/2}$, where k_B is the Boltzmann constant, and m is the mass of carbon atom.

For LS-contact, both the wide base and the narrow top of the pyramid device interact with each thermal contact through a finite number of atoms. Therefore, a fluctuating net momentum, whose magnitude is proportional to $(T/N_{sub})^{1/2}$, is being transferred from the thermostatted atoms of the reservoir to the device. In the narrow top of the device, 8 or 18 atoms, depending on whether the top area is composed of 2 × 2 unit cells or 3 × 3 unit cells, are covalently bonded to the equal number of thermostatted atoms in Contact2. The number of atoms directly involved in device-contact interaction is so small that the net momentum (whose average over time is zero) transferred from Contact2 to the narrow top is not negligible, which results in collective vibrations of atoms in the narrow region of the device. Because the strength of this fluctuating net COM velocity depends on the reservoir temperature ($\sim\sqrt{T}$), the vDOS of the narrow top is rather sensitive to the temperature change. On the contrary, in the wide base of the pyramid device, 512 atoms are covalently bonded to Contact1 atoms. The sufficiently large number of atoms participating in the device-contact energy exchange average out the net velocity transferred to the device from the contact, rendering vDOS less sensitive to the temperature change.

The wide base and narrow top are simply two different regions in a single device, separated by 9 unit cells (∼ 4 nm), therefore a trace of the low-frequency vibration peaks found in the narrow top region can still be found in the wide base vDOS at the same frequencies (Figure 4b). However, the intensity of these peaks is significantly reduced in the wide base vDOS, indicating that the wide base is not as susceptible to the collective low-frequency vibrations as the narrow top. It is because of the much larger number of thermostatted atoms in Contact1 at the lower temperature effectively suppressing the excitation of the COM motion of the wide base through the device-reservoir interaction. The difference between the wide base and the narrow top in the susceptibility to COM motion renders the low-frequency COM vibrations to be localized standing waves in the narrow top region, as indicated by sharp peaks in the narrow top vDOS in Figure 4b. Such a mismatch in vDOS results in a reduced heat flux, because the thermal energy accumulated in the low-frequency vibration modes of narrow top cannot be efficiently transferred to the wide base, unless converted to other vibration modes shared between the two sides. The additional dissipation process of the mismatched vibrations of the narrow top slows down the heat flux when Δ is negative.

Although the nonuniform vDOS with varying temperature dependency makes any quantitative prediction of the device heat capacity a very challenging task, especially in the presence of a strong temperature gradient across the system, it still provides qualitative insights crucial for understanding the mechanism behind the thermal rectification of the shape asymmetric nanodevice. From above discussion, it now becomes intuitively apparent that the device with a lesser degree of shape asymmetry should exhibit a weaker thermal rectification, as depicted in Figure 3b, because the lessened difference in the atomic degrees of freedom participating in the device-contact interaction at both ends of the device decreases the difference in the strength of statistical fluctuation ($\sim N^{-1/2}$).

In LS-contact, all the atoms in both top and bottom surfaces of the device are interacting with the thermal reservoirs. It was discussed that the difference in the number of device atoms due to the shape asymmetry results in the difference in the temperature dependency of vDOS, which breaks the symmetry of the heat flux. In the following discussion of SS-contact, the number of contact atoms directly interacting with the thermostat is controlled not by the shape of the device but by the size of the thermal reservoir. It is demostrated that although the wide base of the device has a sufficiently large number of surface atoms, the vDOS of the wide base becomes susceptible to the increased fluctuation, because only a fraction

dx.doi.org/10.1021/nl301006y | Nano Lett. XXXX, XXX, XXX−XXX

of them (through which thermal energy exchange occurs) are covalently bonded to the thermostatted atoms of Contact1. Therefore, a qualitatively different outcome follows when the size of thermal contacts are modified from LS-contact to SS-contact.

As shown in Figure 6a, the heat flux in SS-contact reduces considerably compared to LS-contact case, when Δ is positive.

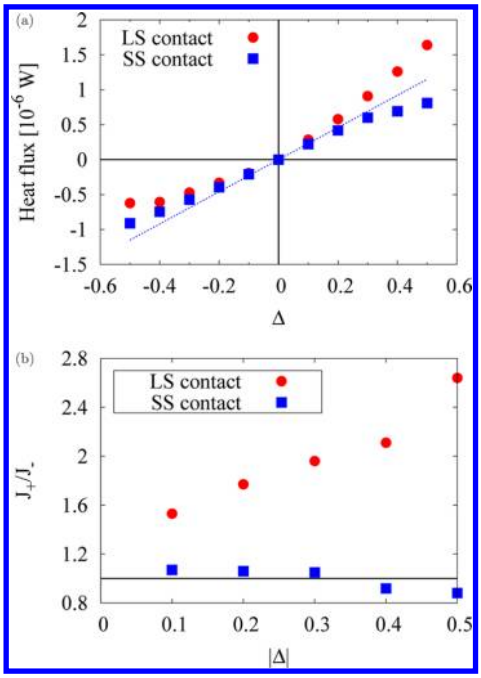

Figure 6. SS-contact case is compared with LS-contact case. The device between contacts has the 2 × 2 unit cells top in both cases. (a) SS-contact case shows weaker heat flux compared to LS-contact case when Δ is possive. (b) SS-contact shows very weak thermal rectification. The direction of rectification changes when |Δ| is large. Errors are smaller than the size of symbols.

On the other hand, a slight increase in the magnitude of heat flux is observed for negative Δ. Consequently, the magnitude of the thermal rectification decreases dramatically and even reverts its direction, when |Δ| is large (Figure 6b). The negligible magnitude of rectification, along with its switching direction, makes SS-contact an impractical setting for a thermal rectification. It is the symmetry of the thermal contacts at both ends of the pyramid device, that is, the equal number of atoms involved in device-contact interaction at both ends, that almost deprives the shape asymmetric device of its thermal rectifying property. Because the major difference in the heat flux between LS-contact and SS-contact occurs when Δ is positive and large, Figure 7 compares the vDOS of the wide base region between LS-contact and SS-contact when both systems have a Δ of +0.5.

A drastic change in the vibrational characteristics is observed in the wide base of the pyramid device when the contact configuration is changed from fully thermostatted (LS) to partially thermostatted (SS). In SS-contact, as the wide surface of the pyramid device is only partially supported by a much smaller reservoir, four unsupported/unthermostated corner regions are subjected to the low-frequency tip vibrations, whose magnitude strongly depends on temperature. In experiments, it is a well-known fact in STM or AFM that the magnitude of the low-frequency probing tip vibration is sensitive to the ambient

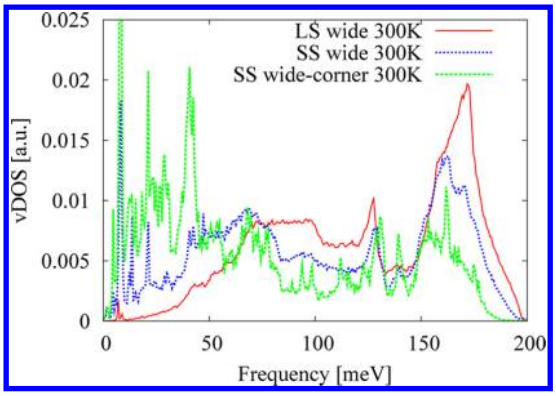

Figure 7. The red line is the vDOS of wide base region of the device in LS-contact when Δ = +0.5. The blue line is the vDOS of wide base region of the device in SS-contact when Δ = +0.5. The green line shows the vDOS in the corner parts of the wide bottom of the device, which are not atached to the thermostat. The device between contacts has 2 × 2 unit cells top.

temperature, thereby affecting their spatial resolution. This is confirmed in Figure 7, which shows that the drastic change in vDOS of the wide base in SS-contact is primarily due to the low-frequency vibrations of unthermostated corner tips. On the contrary, as shown in Figure 4a, the vibrations of the narrow top do not include such strong low-frequency modes, despite the small number of contact atoms, when the temperature of Contact2 is as low as 100 K (Δ = +0.5). The reduced heat flux of SS-contact at large positive Δ is due to inefficient transport of the thermal energy, accumulated in the low-frequency vibrations of the wide base, to the narrow top. The consequence of this inefficient transport at large positive Δ is reflected in the observation of opposite rectification feature (Figure 6b).

The investigation of the thermal rectification features in the LL-contact case, where a large Contact2 is attached to the narrow side of the device, presents a delicate numerical issue. In terms of the number of atoms participating in the heat exchange between the narrow top of the device and Contact2, the LL-contact case is identical to the LS-contact case (Figure 2a,c). In the LL-contact case, however, as the heat flows through a narrow area between the device and Contact2, the steady state temperature field within Contact2 evolves as severely nonuniform, although the spatially averaged overall temperature of Contact2 is thermostatted at a fixed value. The nonuniform temperature profile within Contact2 always renders a reduced temperature difference between the two ends of the pyramid device, which in turn results in a reduced heat flux along the device. Therefore, the magnitude of the thermal rectification in LL-contact is not as strong as that of LS-contact. However, when additional smaller thermostats are added within Contact2 to enforce temperature uniformity across Contact2, the thermal rectification increases with reinforced temperature gradient, similar to what is found in the LS-contacts (Figure 8a,b).

In conclusion, using simulation studies on pyramid-shaped diamond nanostructures, we show that thermal rectification in asymmetric low-dimensional nanostructures can be generalized to three-dimensional materials. Furthermore, we show that the performance of the thermal rectifier strongly depends on the size of the thermal contacts. Our study suggests that the thermal rectification in the size-asymmetric nanodevice with asymmetric thermal reservoirs (i.e., LS-contact) results from

dx.doi.org/10.1021/nl301006y | Nano Lett. XXXX, XXX, XXX−XXX

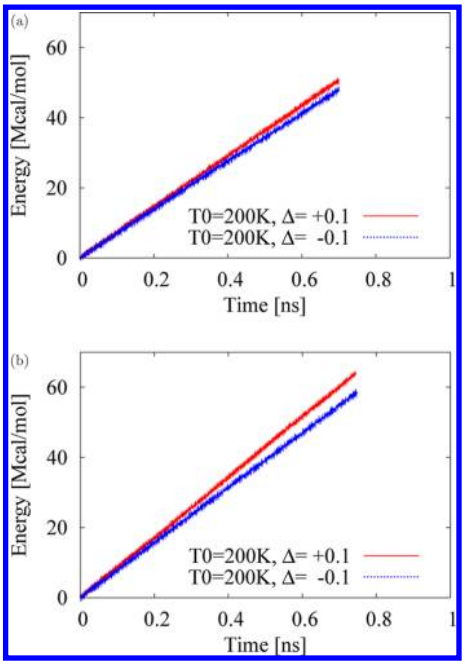

Figure 8. The total amount of thermal energy added to (or removed from) the Contact1 of LL-contact to maintain its temperature is plotted against the simulation time in the steady state, where the same amount of energy is removed from (or added to) Contact2. The slope corresponds to the heat flux, J. (a) J_+, the slope when $\Delta>0$, is slightly higher than J_-, the slope when $\Delta<0$. (b) Both J_+ and J_- increase, when additional small thermostat patche is used to ensure the uniform temperature in Contact2. J_+ becomes noticeably higher than J_-, indicating enhanced thermal rectification. The pyramid device with 3 × 3 unit cells top is used (Figure 1a).

the stronger temperature dependence of the narrower region's vibration density of states (vDOS), which results in noticeable vDOS mismatch between the two end regions of the device when the narrow end is thermostatted at the higher temperature. The asymmetry in the temperature dependency of the regional vDOS originates from the difference in the number of atoms participating in the device-contact interaction at both ends for thermal energy exchange. When a small number (N_{sub}) of atoms are involved in the device-thermostat interaction, non-negligible fluctuating net momentum ($\propto(T/N_{sub})^{1/2}$) is transferred to the device from the thermostat. The difference in N_{sub} at both ends of the device eventually breaks the heat flux symmetry when the temperature bias is reversed. The current study identifies the asymmetry in vDOS temperature dependency as a key feature that is necessary for noticeable thermal rectification in 3D nanostructures. The required asymmetry in vDOS, which utilizes the difference in the number of thermosttated device atoms, can also be realized using partial thermostatting (clapping) of the nanodevice without relying on the device shape asymmetry. In fact, Gordiz et al. applied asymmetric thermostat on size-symmetric multiwalled CNT and observed noticeable thermal rectification.[14]

AUTHOR INFORMATION

Corresponding Author

*E-mail: jonghoon.lee@wpafb.af.mil.

Notes

The authors declare no competing financial interest.

ACKNOWLEDGMENTS

The authors are grateful to U.S. Air Force Office of Scientific Research (AFOSR) and Dr. Byung-Lip Les Lee for the financial support under Lab Task:2302BR7P, Department of Defense Supercomputing Research Center (AFRL-DSRC) for computational time to carry out the simulations. and Dr. Jennifer Wohlwend for the critical reading of this letter.

REFERENCES

(1) Chang, C. W.; Okawa, D.; Majumdar, A.; Zettl, A. *Science* **2006**, *314*, 1121.
(2) Roberts, N. A.; Walker, D. G. *Int. J. Therm. Sci.* **2011**, *50* (5), 648.
(3) Hu, J.; Ruan, X.; Chen, Y. *Nano Lett.* **2009**, *9*, 2430.
(4) Yang, N.; Zhang, G.; Li, B. *Appl. Phys. Lett.* **2009**, *95*, 033107.
(5) Wu, G.; Li, B. *J. Phys.: Condens. Matter* **2008**, *20*, 175211.
(6) Yang, N.; Zhang, G.; Li, B. *Appl. Phys. Lett.* **2009**, *93*, 243111.
(7) Alaghemandi, M.; Leroy, F.; Algaer, E.; Bohm, M.; Muller-Plathe, F. *Nanotechnology* **2010**, *21*, 075704.
(8) Plimpton, S. *J. Comput. Phys.* **1995**, *117*, 1.
(9) Sun, H.; Mumby, S. J.; Maple, J. R.; Hagler, A. T. *J. Am. Chem. Soc.* **1994**, *116*, 2978.
(10) Varshney, V.; Roy, A.; Dudis, D.; Lee, J.; Farmer, B. L. A novel nano-configuration for thermoelectrics: Helicity induced thermal conductivity reduction in nanowires. *Nanoscale*, DOI: 10.1039/C2NR30602F.
(11) Bosak, A.; Krisch, M. *Phys. Rev. B* **2005**, *72*, 224305.
(12) Harvey, S.; Tan, R. K. Z.; Cheatham, T. E. *J. Comput. Chem.* **1998**, *19*, 726.
(13) Landau, L.; Lifshitz, E. *Statistical Physics, Part. 1*; Butterworth-Heinemann: Woburn, MA, 1980.
(14) Gordiz, K.; Allaei, S. M. V.; Kowsary, F. *Appl. Phys. Lett.* **2011**, *99*, 251901.